Available online at www.sciencedirect.com
ScienceDirect
Infrared Physics & Technology xxx (2007) xxx–xxx
INFRARED PHYSICS & TECHNOLOGY
www.elsevier.com/locate/infrared

Band pass filters in the 1 μm spectral region: Thick metal screens

A. Lüker [a,1], H. Hein [a], J. Schulz [a], N. Dambrowsky [a], O. Sternberg [b], M.J. Sweetgall [b,c], K. Abdijalilov [b,d], K.D. Möller [b,d], H. Grebel [b,d,*]

[a] Forschungszentrum Karlsruhe, Institut für Mikrostrukturtechnik, Postfach 3640, Karlsruhe 76021, Germany
[b] Electronic Imaging Center, New Jersey Institute of Technology, Newark, NJ 07102, USA
[c] Bergen County Academies, Hackensack, NJ 07601, USA
[d] Electrical Engineering Department, New Jersey Institute of Technology, Newark, NJ 07102, USA

Received 25 January 2007

Abstract

Free standing metal screens have long been used as band pass filters in the infrared (IR) wavelength region. One adjusts the screens' periodicity constant, its opening-to-periodicity aspect ratio and its thickness to achieve desired infrared transmission properties. Here we concentrate on thick screens in the near IR wavelength region (1–2 μm). In addition to experiments and simulations we have considered the role of screen imperfection on its transmission characteristics. Uneven surfaces, inclined and sometimes rough walls of the screen and waveguide channels may be the result of thick-film lithography which is used in the process for screen manufacturing. Understanding these effects is crucial to applications of these filters in the entire IR region.

Keywords: Resonance screen; Inductive screens; Infrared filters; Imperfect manufacturing

1. Introduction

Free standing metal screens have been studied in the long [1,2] and short [3] wavelength regions. Transmittances of screens with various aspect ratios (opening-to-periodicity ratio) have been investigated from the visible to the THz spectral regions. Resonances of the screens may be interpreted in terms of surface plasmons/waves [4–7] and waveguide modes [8,9]. Surface plasmons terminology is commonly used when complex refractive index parameters are employed [10] whereas surface waves terminology is used when surface impedance boundary conditions [11] are applied.

Free standing metal screens have been traditionally used by the astrophysical community in the longer wavelength region; [1] applications in the short wavelength region though, have been limited by the manufacturing screen process. Thick screens, with ratio of thickness-to-lattice periodicity larger than unity, tend to portray inclined or curved walls, rounding of the ends of the openings and unevenness of the screen surfaces. In this paper we report on transmittance properties of free standing Au screens for the 1–2 μm wavelength region with waveguide channels which are arranged in square and hexagonal lattices. Variations in the screen features may be in the range of tens or even hundreds of nanometers despite the best lithographical tools used and their impact on their transmittance characteristics should therefore be considered. In addition to study ideal screens we analyzed imperfect ones by use of coupled wave model [8,9]. We obtained agreement between the model and experimental data and attributed the difference between simulations and experimental data to random (inhomogeneous) screen imperfections.

* Corresponding author: Address. Electrical Engineering Department, New Jersey Institute of Technology, Newark, NJ 07102, USA. Tel.: +1 973 596 3538.
E-mail address: grebel@njit.edu (H. Grebel).
[1] Present address: Microsystems and Nanotechnology Centre, School of Applied Sciences (SAS), Cranfield University, Cranfield, Bedfordshire MK 43 0AL, United Kingdom.

1350-4495/$ - see front matter © 2007 Elsevier B.V. All rights reserved.
doi:10.1016/j.infrared.2007.07.007

2. Experiments

Inductive metal screens are shown in Fig. 1a and b. Two sets of metal screens were made of gold: square shaped waveguide channels with rectangular symmetry and hexagonal waveguide channels with hexagonal symmetry. The periodicity constant g was aimed at 1.3 μm and the thickness of the waveguide channels at 2.3 μm. Experimental values for the periodicity constant g and the waveguide channels' thickness values t and the opening dimension D_1 and D_2 on either side of the screen are given in Table 1. The screens were placed on another metal frame which had openings of 50 μm, wire size of 5 μm and thickness of 2.3 μm. The overall sample area was 6–10 mm^2. Samples were prepared by use of 100 KeV e-beam lithography and electro deposition without a seed layer. Heavily n-doped silicon wafers with a specific resistively of 0.01–0.02 Ω-cm were used as substrates for the freestanding metal LIGA-based structures. Each substrate was coated with 3 μm positive electron-beam resist (PMMA-950 K with 11% solids in Anisole). After exposure and spray-development for 2.5 min in a 1:1 methylisobutylketone:isopropylic alcohol (MIBK:IPA) mixture, a descum step, aim at removing residual resist layers from the substrate, was performed. The native silicon oxide was removed by use of 5% HF solution prior to the electroforming stage. Ti contact clamps were used as contacts for the electro deposition process. The contact potential difference between the titanium and the n-doped silicon was almost ohmic due to the small relative electron work function of titanium (with the exception aluminum, a Schottky-contact with n-doped silicon is typically developed, which upon application of cathodic potential for the plating process, becomes reverse biased). Initial high-nucleation density was achieved by using current density of 0.8 A/dm^2 for the first 5 s; tests with lower current densities did not result in a homogenous layer formation. To ensure stability of the electrolyte, the pH of the plating solution was kept between 8 and 9. After resist stripping, the deposited structures were released by simple anisotropic etching in 30% KOH for 5 min at near room temperature.

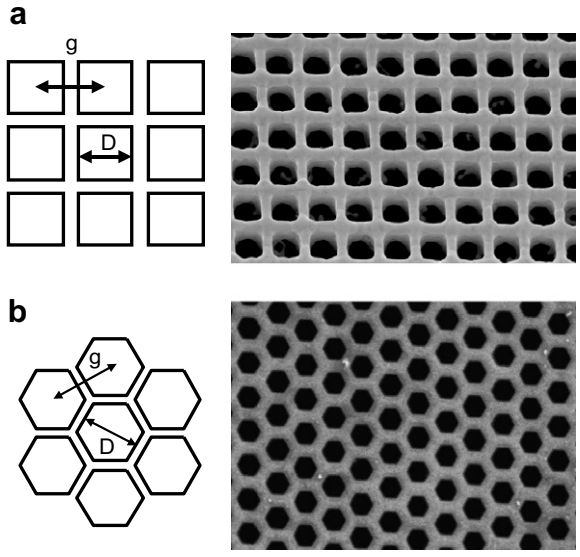

Fig. 1. (a) Rectangular periodic structure with square shaped waveguide channels; the periodicity constant is g and the waveguide opening D. (b) Hexagonal structure with hexagonal shaped waveguide channels; the periodicity constant is g and the waveguide opening D.

3. Theoretical considerations

Surface waves, propagating on either screen's surface are coupled by waveguides modes, either propagating or evanescent, in the screen's waveguide channel. Taking x and y coordinates in the plane of the screen and z for the normal direction, waveguide modes are denoted by TE (the electric field has no component in the z-direction) and TM (the magnetic field has no component in the z-direction). Typically, resonances in the screen are associated with incident beams as p-polarized (electrical vector in the plane of incidence) and s-polarized (electrical vector normal to the plane of incidence) [12]. Dispersion relations dictate that the propagation constant of the surface wave k_s is related to the periodicity g and the propagation constant of the incident beam k_0 by, $(k_{sx})^+ = k_0 \sin(\theta) + q2\pi/g$ and $(k_{sx})^- = k_0 \sin(\theta) - q2\pi/g$, with q, integer. Resonance occurs whenever the propagating surface wave becomes a standing wave, thus, for normal incidence ($\theta = 0$), $\mathbf{k}_s = (k_{sx})^+ + (k_{sx})^- = 0$. There are surface waves on either side of the screen, coupled through the opening via waveguide (either propagating or evanescent) modes [8,9]. For metals, $k_s = k_0(\varepsilon_m\varepsilon_0/\varepsilon_m + \varepsilon_0)^{1/2}$ with ε_m, the dielectric constant of metal and ε_0, the dielectric constant of air or a dielectric filling. For ideal metal, $\varepsilon_m \ll 0$ and $k_s \sim k_0$. When the metal is perforated and the holes are filled with a dielectric material, the effective dielectric constant is $\varepsilon_{eff} = A_m\varepsilon_m + A_d\varepsilon_d$, with A_m, A_d, the areas occupied by the metal and dielectric, respectively. Since $\varepsilon_m \ll 0$ and ε_d is a relatively small positive number, ε_{eff} is also a large negative number which implies $k_s \sim k_0$ at normal incidence as well. The compound

Table 1
Periodicity constants, opening diameters and thickness of screens

		g	D_1	D_1/g	D_2	D_2/g	t	t/g
S1	Square, rectangular	1.3	1	0.77	0.9	0.69	2.3	1.77
S2	Square, rectangular	1.28	1	0.78	0.8	0.63	2.3	1.80
H1	Hexagonal, hexagonal	1.24	1	0.81	0.7	0.56	2.3	1.85
H2	Hexagonal, hexagonal	1.28	0.7	0.55	0.5	0.39	2.3	1.80

Please cite this article in press as: A. Lüker et al., Band pass filters in the 1 μm spectral region: Thick metal screens, Infrared Phys. Techn. (2007), doi:10.1016/j.infrared.2007.07.007

mode of the coupled surface wave and its resonances are our focus of attention.

4. Experimental and simulated results

Transmittances through rectangular structures S1 and S2 (Fig. 2) portray a dominant peak at wavelength near 1.8 μm and a number of smaller side peaks on the shorter wavelength region. The hexagonal structure H1 has a dominant peak at wavelength near 1.7 μm. We used coupled surface wave model and simulations with the Micro-Stripes program to analyze these screens. Similarly to the experiments, simulations have identified several side peaks which overlap with the dominant peak: this was true for both rectangular and hexagonal structures, shown in Fig. 3 for square shaped screens. This is also in contrast to cross-shaped screens where the side peaks are well separated from the main one. These peaks are labeled α, β, γ and δ from the long wavelengths down and are attributed to the longitudinal resonances (Fig. 4). Thin screens exhibit only the zero-order waveguide mode, α. As the thickness of the screen increases the waveguide supports second- and third-order longitudinal waveguide modes, β, γ, and δ as schematically shown in Fig. 4. Experimental transmission spectra, however, for both structures (Fig. 2) do not exhibit much of the first- to third-order waveguide modes (β, γ, and δ). *Our hypothesis is that the difference between the simulated and experimental spectra has its origin in homogeneous, yet, small imperfections, which were introduced by the manufacturing process to all screens features alike*.

In order to include *homogeneous* sample imperfections (namely, applied simultaneously to each channel) we repeated the simulations with various conductivity values and effective geometrical features. For the hexagonal structure, simulations have shown little transmission difference between round holes and hexagonal waveguide channels, which may ease the comparison between our results and those reported in the literature (Table 2).

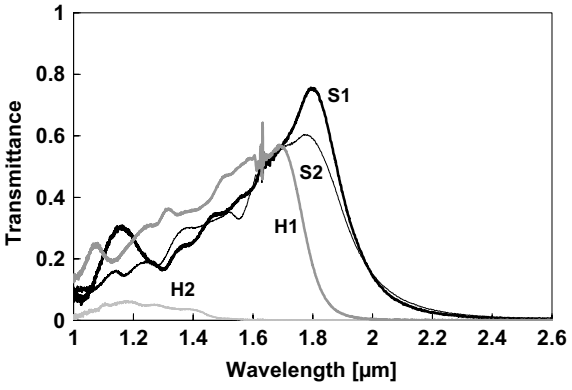

Fig. 2. Transmittance of square shaped waveguide channels in rectangular structure (S1, S2) and hexagonal waveguide channels in hexagonal structure (H1, H2). Periodicity constants and waveguide dimensions are given in Table 1. The spectral features at 1.6 μm are artifacts of the spectrometer.

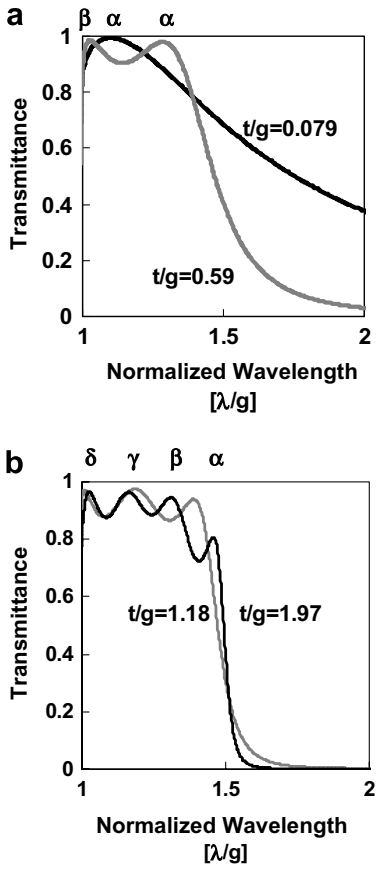

Fig. 3. Simulations: waveguide modes in square-shaped sample with rectangular structure as a function of normalized wavelength λ/g for various thickness values t. (a) Ratio of thickness to periodicity constant $t/g = 0.079$ and 0.59; (b) $t/g = 1.18$ and 1.97. For a definition of α, β, γ, and δ modes, see Fig. 4.

Fig. 4. Nodes of the compound mode as a function of thickness. Thin screens exhibit no node. As the screen thickness increases the channel supports more and more nodes.

4.1. Screens with rectangular symmetry

In Fig. 5 we provide comparison between simulations for ideal screens with perfect waveguide channels and infinite conductivity values and simulations for Au and Ni perfect screens (straight walled yet, with finite conductivity values). The smaller conductivity values affect the intensity of the zero-order waveguide modes more than the higher-order ones. In Fig. 6 we considered Au screens with conical shaped waveguide channels. Here, no reduction in the intensity of the higher-order waveguide mode and suppression of the lower-order modes is noted. At the same time

Please cite this article in press as: A. Lüker et al., Band pass filters in the 1 μm spectral region: Thick metal screens, Infrared Phys. Techn. (2007), doi:10.1016/j.infrared.2007.07.007

Table 2
Geometrical parameters, observed, cut-off and calculated transmittance wavelength

					$\lambda_p = 0.9g + 0.22D$		
					Observed		$\lambda_c = 1.71D$
		D	g	t	WL	cal.	Cut-off
Ref. [13]	Round	1400	1600	3000	1900	1748	2389.1
Ref. [16], #1	Round	168	226	153	230	240.36	286.7
Refs. [16,8]	Hex	88	179	88	176	180.46	150.2
Ref. [14], 155	Round	111	164	70	172	172.02	189.4
Ref. [14], 215	Round	77	118	55	122	123.14	131.4
Ref. [14], 275	Round	52	92	55	93	94.24	88.7
Ref. [14], 355	Round	37	72	52	70	72.94	63.1
Ref. [15]	Round	8	12	Not aval.	11	12.56	13.7
Ref. [15]	Round	5	7.5	Not aval.	7.5	7.85	8.5
Ref. [15]	Round	1.7	2.55	Not aval.	2.8	2.669	2.9
Ref. [15]	Round	1.2	1.8	Not aval.	2	1.884	2.0
H1	hex	1	1.24	2.3	1.7	1.336	1.7
Ref. [15]	Round	0.9	1.35	Not aval.	1.6	1.413	1.5
Ref. [15]	Round	0.6	0.9	Not aval.	1.05	0.942	1.0
Ref. [15]	Round	0.35	0.525	Not aval.	0.7	0.5495	0.6
Ref. [15]	Round	0.23	0.345	Not aval.	0.4	0.3611	0.4
							$\lambda c = 1.41D$
S1	Square	1	1.3	2.3	1.8	n.a.	1.41

D, diameter of opening; g, periodicity constant; t, thickness; WL, observed peak wavelength; cal., calculated peak wavelength; cut-off, cut-off wavelength.

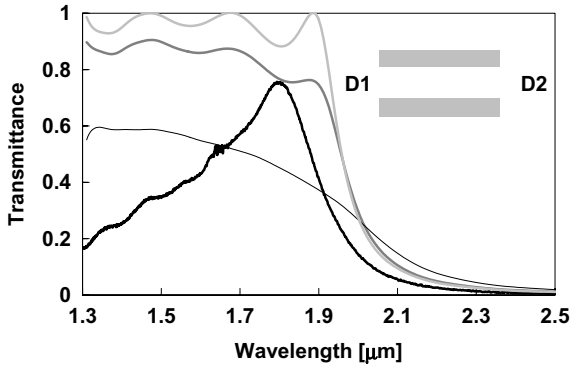

Fig. 5. Simulated transmittances for square shaped structures with perfect waveguide channels, $D_1 = D_2 = 1$ μm and various conductivity values. Light gray: ideal case (infinite conductivity). Dark gray: Au. Thin black: Ni. Experimental data for screen S1: bold black.

one finds that the peaks shift to shorter wavelengths for smaller values of D_2. A neck shaped waveguide channel (Fig. 7) exhibited no reduction in the appearance of waveguide modes. It shifted the modes to the shorter wavelength regime and accentuated the cut-off wavelength.

The above waveguide modifications have well defined geometry and conductivity values. Yet, inspection of the back-side of the rectangular latticed screens with an electron microscope revealed irregular metal surface with small cylindrical features. We note that Fig. 7 indicates that only a small neck is required to mimic a sharp wavelength cut-off. A small cylinder at the back side of a neck-shaped channel ($D_1 = D_2 = 1$ and $D_m = 0.95$) and shown in inset of Fig. 8, was added to the simulation structure in order

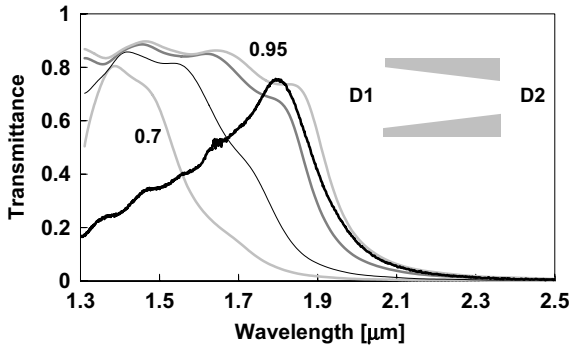

Fig. 6. Simulated transmittance for square shaped structure with conical shaped waveguide channels made of Au. All dimensions are in micrometers and all having $D_1 = 1$. Light gray: $D_2 = 0.95$. Dark gray: $D_2 = 0.9$. Thin black: $D_2 = 0.8$. Light gray: $D_2 = 0.7$. Experimental data for screen S1: bold black.

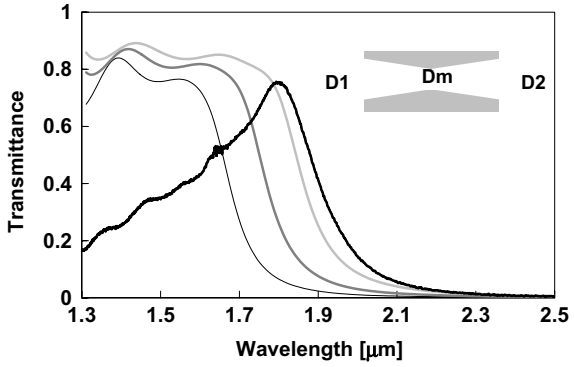

Fig. 7. Simulated transmittance for square shaped structure with neck shaped waveguide channels, all dimensions are in micrometers. Light gray: $D_1 = 1$, $D_m = 0.9$, $D_2 = 1$. Dark gray: $D_1 = 0.95$, $D_m = 0.85$, $D_2 = 0.95$. Thin black: $D_1 = 1$, $D_m = 0.85$, $D_2 = 1$. Experimental data for screen S1: bold black.

Please cite this article in press as: A. Lüker et al., Band pass filters in the 1 μm spectral region: Thick metal screens, Infrared Phys. Techn. (2007), doi:10.1016/j.infrared.2007.07.007

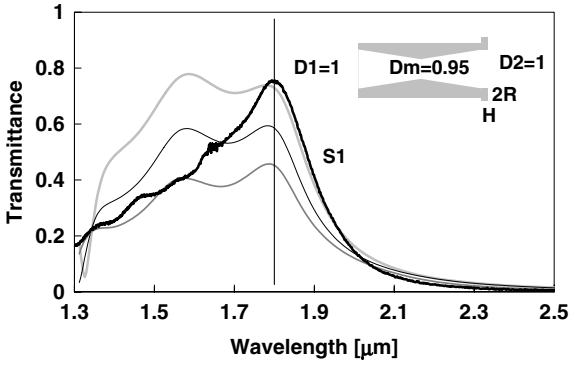

Fig. 8. Simulated transmittance for square shaped structure with uneven back surface represented by neck shaped waveguide channel with small cylinders, all in micrometers. Neck shape: $D_1 = 1$, $D_m = 0.95$, $D_2 = 1$. Cylinders: light gray: $H = 0.3$, $R = 0.5$. Dark gray: $H = 0.3$, $R = 0.6$. Thin black: $H = 0.3$, $R = 0.7$. Experimental transmittance data for screen S1: bold black.

to account for such uneven surface. Simulations were performed for various radii R and heights H of the cylinders, keeping the total length of the neck shaped channel and cylinder height at 2.3 μm. As shown in Fig. 8, all simulations exhibited reduction in the intensity of higher-order waveguide modes, and a good agreement between the experimental and simulated values for the *zero-order mode* peak.

4.2. Screens with hexagonal symmetry

Similar results were obtained for hexagonal shaped screens (Figs. 9 and 10). The higher-order waveguide modes were only little affected by the various geometries of the waveguide channels and so were the results with various conductivities values (Fig. 11). We have not considered here cylindrical shape features as for the rectangular cases since such imperfection were not found upon inspection with the electron microscope.

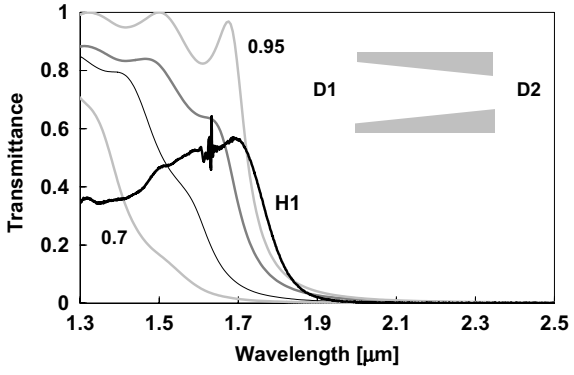

Fig. 9. Simulated transmittance for hexagonal shaped structure (Au) with cone shaped waveguide channels, all in micrometers. All $D_1 = 1$, Light gray: $D_2 = 0.95$. Dark gray: $D_2 = 0.9$. Thin black: $D_2 = 0.8$. Dark gray: 0.7. Experimental transmittance data for screen H1: bold black.

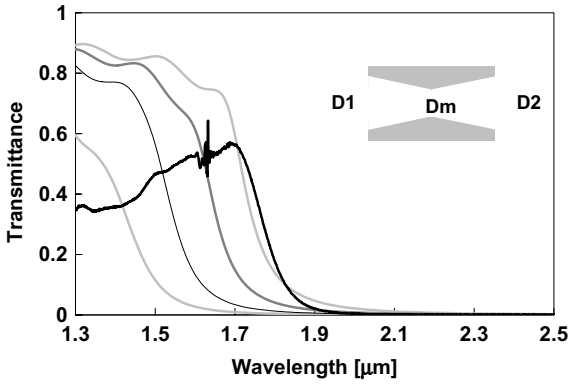

Fig. 10. Simulated transmittance for hexagonal shaped structure with neck shaped waveguide channel channels, all in micrometers. Light gray: $D_1 = 1$, $D_m = 0.95$, $D_2 = 1$. Dark gray, $D1 = 1$, $D_m = 0.9$, $D_2 = 1$. Thin black: $D_1 = 1$, $D_m = 0.8$, $D_1 = 1$. Light gray: $D_1 = 1$, $D_m = 0.7$, $D_2 = 1$. Experimental transmittance data for screen H1: bold black.

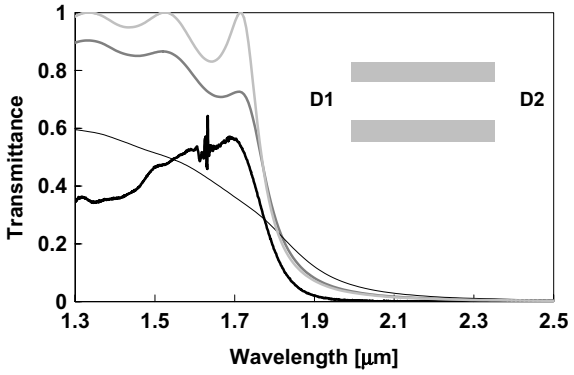

Fig. 11. Simulated transmittances for different conductivities of hexagonal shaped structure with straight waveguide channels $D_1 = D_2 = 1$ μm. Light gray: no loss. Dark gray: Au. Thin black: Ni. Experimental transmittance data for screen H1: bold black.

5. Discussion

The transmission spectra of thick free standing screens exhibit one dominant peak λ_p with steep transmission reduction at longer wavelength in addition to side peaks on the shorter wavelength range. Similar peak spectra have been reported in the past for many hexagonal structures as we discuss below. The steep cut-off at the long wavelengths was assigned to the cut-off wavelength λ_c of a single waveguide [13]: by definition, $\lambda_c > \lambda_p$. Studies of λ_p and λ_c for screens in the visible to the mm wavelength region reveal that the relation $\lambda_c > \lambda_p$ does not hold for some experiments with hexagonal structures, [14] and is not held true for square shaped screens. Our simulations reveal that the peak transmission wavelength mainly depends on the periodicity constant (Fig. 12) with little dependence on the opening of the waveguide channels. It is exhibited for hexagonal structures by an empirical relationship: $\lambda_p = 0.9g + 0.22D$. The latter is derived from the experimental data of Table 2 and Refs. [14,15]. It is plotted in Fig. 13 for values of waveguide openings obeying the

Please cite this article in press as: A. Lüker et al., Band pass filters in the 1 μm spectral region: Thick metal screens, Infrared Phys. Techn. (2007), doi:10.1016/j.infrared.2007.07.007

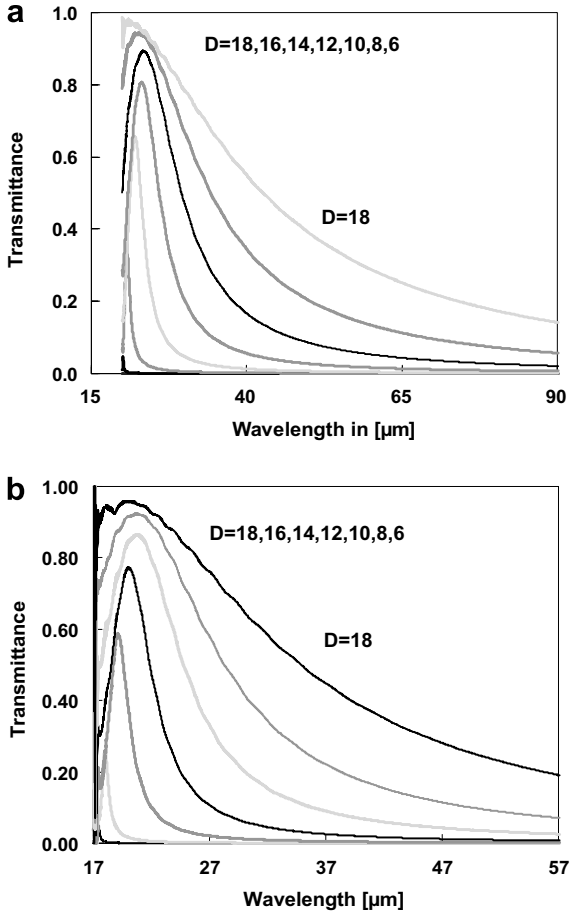

Fig. 12. Simulations of resonance wavelength for screens with fixed periodicity constant $g = 20$ μm. (a) Square shaped screens, as a function of screen opening $D = 18$–6 μm. (b) Hexagonal shaped screens, as a function of screen opening $D = 18$–6 μm.

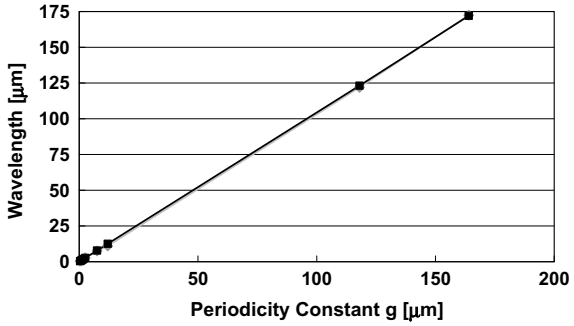

Fig. 13. Hexagonal structure: transmission wavelength as a function of periodicity constant with $D = 0.7g$. Black: empirical formula, $\lambda_p = 0.9g + 0.22D = 1.054g$. Gray: experimental data.

relationship, $D = 0.7g$. We note that the empirical relationship for λ_p describes well the position of the main peak for many octaves of wavelengths. The dependence of the peak wavelength on the waveguide opening when both normalized by the periodicity constant g, $\lambda_p/g = 0.9 + 0.22D/g$, appears to be small yet, linear for all data of Table 2 (Fig. 14), as well.

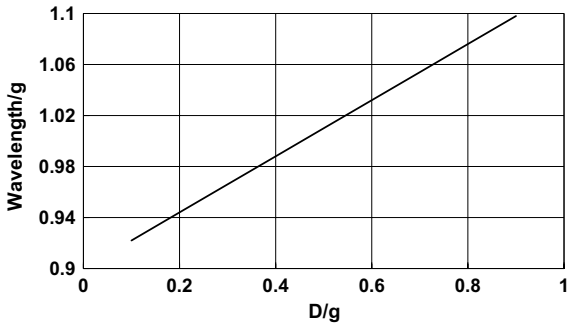

Fig. 14. Peak wavelength divided by the periodicity constant (PWL/g) as a function of channel opening divided by the periodicity constant (D/g) for hexagonal screens. The empirical graph is (PWL/g) = 0.9 + 0.22(D/g).

A difference between experimental and simulated data is noted when considering the entire transmittance curve. Higher-order modes are all but missing from the experimental data. One may also note that simulations indicate a higher-order peak-shift towards the shorter wavelengths as the conical shape becomes more acute (Fig. 6). In addition, it seems that the necking of the waveguide accentuate the cut-off wavelength (Fig. 7) though shifts the peak intensities to the shorter wavelength region. These may be attributed to two different effects: conical shapes eliminate lower-order modes (such as the α mode) at the waveguide end. A neck in the guide divides it into two sections, each supporting a fewer modes in addition to suppressing lower-order modes. Fig. 8 indicated that one requires tempering with the geometrical structure at the screen back in order to suppress the higher-order modes. We chose the neck shape waveguide structure because it retains the lower-order modes with sharp wavelength cut-off. Only a small neck is required to retain the long wavelength part of the transmission spectra while the uneven back surface affects the short wavelength part. However, as the back features become larger, the overall transmittance is reduced and the quality of the filter is compromised.

Our simulation method could not account for randomly distributed differences in geometry and conductivity on a waveguide-by-waveguide basis (defined here as inhomogeneous imperfections, which is in contrast to an overall homogenous change for all waveguides). On the other hand, our manufactured hexagonal shaped screens did not exhibit noticeable surface irregularities – its high-order mode transmittance was suppressed nonetheless. Experimental study in the short wavelength region for hexagonal structures, which were produced by a mechanical manufacturing process, exhibited one dominant peak in addition to small side peaks, much like our hexagonal samples (Fig. 2) [15]. Additional studies [14,16,17] revealed the effect of a 'perfect' versus 'imperfect' manufacturing process. Screens produced by electroforming (the 'imperfect' process) exhibited one main transmission peak whereas, in the same spectral region, the perfect process resulted in transmittance of equal intensity multiple peaks (Fig. 15).

Please cite this article in press as: A. Lüker et al., Band pass filters in the 1 μm spectral region: Thick metal screens, Infrared Phys. Techn. (2007), doi:10.1016/j.infrared.2007.07.007

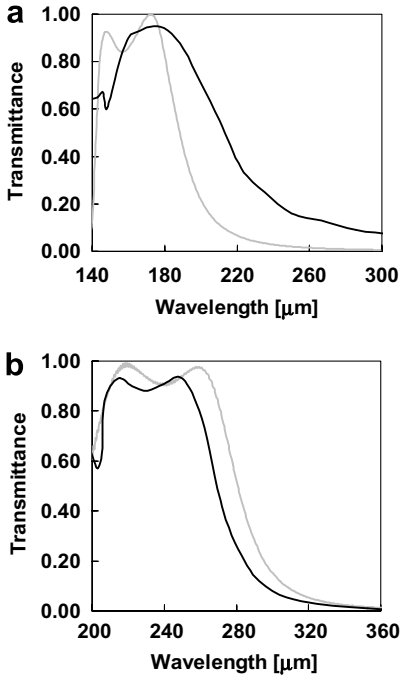

Fig. 15. Comparison between 'imperfect and 'perfect' screens. (a) Commercially electroformed sample ('imperfect') Ni screen with $g = 164$, $D = 111$, $t = 70$. Black: experiment, gray: simulations. (b) A more 'perfect' screen made of brass with $g = 226$, $D = 168$, $t = 153$. Black: experiment, gray: simulations. All dimensions in micrometers.

All of the above considerations require us to estimate the degree of randomly distributed imperfections. Since our model was found adequate from the near IR through the very far IR wavelength region, [9] such estimate may be obtained by comparing a scale-up of our hexagonal samples with a hexagonal sample of round holes and periodicity constant of $g = 1600$ μm, originally designed for the mm wavelength region. In Fig. 16 we compare experimental data for both screens while normalizing the dimensions by the periodicity constant g. As can be seen by the figure, intensity of the high-order channel waveguide modes was reduced for both samples. Mechanical accuracy in the mm scale is on the order of 25 μm or 1–2% of the screen pitch g. This translates to variations of at least 15–25 nm in our samples, much smaller than the propagating wavelength.

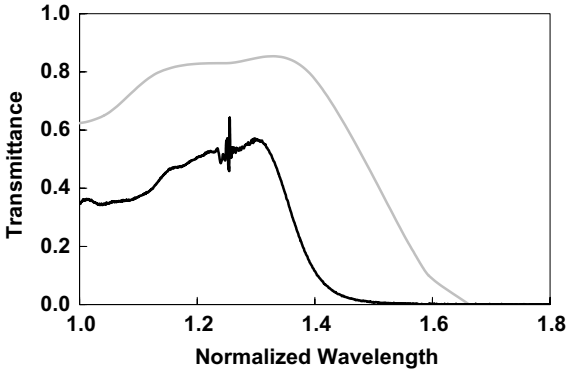

Fig. 16. Comparison between experimental data from a ('perfect') brass screen made in a machine shop and a scaled hexagonal sample of this work. The wavelength was normalized accordingly, λ/g. Gray: $g = 1600$, $D = 1400$, $t = 3000$, and black: $g = 1.3$, $D = 1$, $t = 2.3$. All dimensions are in micrometers.

6. Conclusions

We have studied inductive thick screens with various lattice symmetries and openings. Experimentally we found one major transmission peak whereas simulations exhibited multiple peaks of similar intensity. We identified the peaks by their longitudinal waveguide channel resonances and concluded that the high-order waveguide modes have been suppressed in the experiments. The major peak was well accounted for by simulations and phenomenological approach over many octaves of wavelengths. Attempts to reconcile the difference between experiments and simulations of the high-order modes by varying homogeneously the waveguide geometry and surface conductivity were not satisfying. Thus, we proved false our initial hypothesis that the difference between the simulated and experimental spectra had its origin in homogeneous yet small imperfections. As a consequence we deduced that inhomogeneous imperfections (local random variations) are more important than homogeneous variations (variations which apply to all waveguides alike) in explaining the suppression of higher-order transmission modes in thick inductive screens.

Acknowledgement

This research was sponsored in part by NSF, contract number IIS 0552155.

References

[1] R. Ruprecht, W. Bacher, P. Bley, M. Harmening, W.K. Schomburg, KfK-Nachr. Jahrg. 23 (1991) 2–91, 18–123.
[2] B.J. Munk, Frequency Selective Surfaces, John Wiley & Sons, Inc., New York, 2000.
[3] D.E. Grupp, H.J. Lezec, T.W. Ebbesen, K.M. Pellerin, T. Thio, Crucial role of metal surface in enhanced transmission through subwavlength apertures, Appl. Phys. Lett. 77 (2000) 1569–1571.
[4] R. Ulrich, Modes of Propagation on an Open Periodic Waveguide for the Far Infrared, Microwave Research Institute Symposium Series, vol. XXIII, Polytechnic Institute of New York, NY, 1974.
[5] L. Martin-Moreno, F.J. Garcia-Vidal, H.J. Lezec, K.M. Pellerin, T. Thio, J.B. Pendry, T.W. Ebbesen, Theory of extraordinary optical transmission through subwavelength hole arrays, Phys. Rev. Lett. 86 (2001) 1114–1117.
[6] W.L. Barnes, W.A. Murray, J. Dintinger, E. Devaux, T.W. Ebbesen, Surface plasmon polaritons and their role in the enhanced transmission of light through periodic arrays of subwavlength holes in a metal film, Phys. Rev. Lett. 92 (2004) 107401-1–107401-4.
[7] K.J. Koerkamp, S. Enoch, F.B. Segerink, N.F. Van Hulst, L. Kuipers, Strong influence of hole shape on extraordinary transmission through periodic arrays of subwavelength holes, Phys. Rev. Lett. 92 (2004) 183901-1–183901-4.

[8] C.-C. Chen, Transmission of microwave through perforated flat plates of finite thickness, IEEE Trans. Microwave Theory Tech. 21 (1973) 1–7.
[9] K.D. Möller, O. Sternberg, H. Grebel, P. Lalanne, Thick inductive cross-shaped metal meshes, J. Appl. Phys. 91 (2002) 1–5.
[10] H. Raether, Surface Plasmons on Smooth and Rough Surfaces and on Gratings, Springer-Verlag, Berlin, 1988.
[11] J.D. Jackson, Classical Electrodynamics, 2nd ed., Wiley, New York, 1975.
[12] S. Ramo, Fields and Waves in Communication Electronics, 2nd ed., John Wiley & Sons, New York, 1994.
[13] T. Timusk, P.L. Richaards, Near millimeter wave band pass filter, Appl. Opt. 20 (1981) 1355–1360.
[14] P.G. Huggard, M. Meyringer, A. Schilz, K. Goller, W. Prettl, Far infrared bandpass filters from perforated metal screens, Appl. Opt. 33 (1994) 39–41.
[15] A. Rosenberg, E.A. Bolten, Optical filters consisting of metallic waveguide arrays, J. Opt. Soc. Am. 17 (2000) 1461–1468.
[16] C. Winnewisser, F.T. Lewen, M. Schall, M. Walther, H. Helm, Characterization and application of dichroic filters in the 0.1-3-THz region, IEEE Trans. Microwave Theory Tech. 48 (2000) 744–748.
[17] M. Bozzi, J. Weinzierl, C. Winnewisser, Design, fabrication, and measurements of frequency-selective surfaces, Opt. Eng. 39 (8) (2000) 2263–2269.

Please cite this article in press as: A. Lüker et al., Band pass filters in the 1 μm spectral region: Thick metal screens, Infrared Phys. Techn. (2007), doi:10.1016/j.infrared.2007.07.007